

**MINERAL-ALKALI REACTIONS UNDER DYNAMIC CONDITIONS**

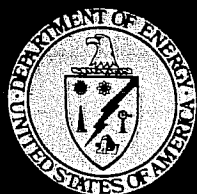
Topical Report

By  
Shawn D. Thornton  
Philip B. Lorenz

November 1988

Performed Under Cooperative Agreement No. FC22-83FE60149

IIT Research Institute  
National Institute for Petroleum and Energy Research  
Bartlesville, Oklahoma



**Bartlesville Project Office  
U. S. DEPARTMENT OF ENERGY  
Bartlesville, Oklahoma**

## DISCLAIMER

This report was prepared as an account of work sponsored by an agency of the United States Government. Neither the United States Government nor any agency thereof, nor any of their employees, makes any warranty, express or implied, or assumes any legal liability or responsibility for the accuracy, completeness, or usefulness of any information, apparatus, product, or process disclosed, or represents that its use would not infringe privately owned rights. Reference herein to any specific commercial product, process, or service by trade name, trademark, manufacturer, or otherwise, does not necessarily constitute or imply its endorsement, recommendation, or favoring by the United States Government or any agency thereof. The views and opinions of authors expressed herein do not necessarily state or reflect those of the United States Government or any agency thereof.

Printed in the United States of America. Available from:

National Technical Information Service  
U.S. Department of Commerce  
5285 Port Royal Road  
Springfield, VA 22161

NTIS price codes

Paper copy: **A03**

Microfiche copy: **A01**

**MINERAL-ALKALI REACTIONS UNDER DYNAMIC CONDITIONS**

**Topical Report**

**By  
Shawn D. Thornton  
Philip B. Lorenz**

**November 1988**

**Work Performed Under Cooperative Agreement No. FC22-83FE60149**

**Prepared for  
U.S. Department of Energy  
Assistant Secretary for Fossil Energy**

**Jerry F. Casteel, Project Manager  
Bartlesville Project Office  
P.O. Box 1398  
Bartlesville, OK 74005**

**Prepared by  
IIT Research Institute  
National Institute for Petroleum and Energy Research  
P.O. Box 2128  
Bartlesville, OK 74005**

MEMORANDUM FOR THE BOARD OF DIRECTORS

Subject: [Illegible]

By: [Illegible]

Date: [Illegible]

1. [Illegible]

2. [Illegible]

3. [Illegible]

4. [Illegible]

## TABLE OF CONTENTS

	<u>Page</u>
Abstract.....	1
Introduction.....	1
Acknowledgments.....	2
Experimental Procedures.....	2
Results.....	4
Alkalinity and pH.....	4
Orthosilicate.....	4
Bicarbonate.....	4
Carbonate.....	5
Magnesium and Calcium.....	5
The Role of Carbon Dioxide.....	8
Oil Production and Permeability.....	10
Conclusions.....	11
Recommendations for Future Research.....	12
References.....	13

## TABLES

	<u>Page</u>
1. Compositions of solutions used in the slim-tube experiments.....	3
2. Sulfate concentrations in bottle-test supernatant.....	7
3. Parameters used in calculations of pH.....	9
4. Calculated vs. measured pH of effluent from slim tube with injection... of $\text{NaHCO}_3$ .....	10
5. Oil production in slim-tube experiments.....	11

## ILLUSTRATIONS

1. Effluent profiles of pH and alkalinity from the slim tube injected with 0.085 N $\text{Na}_4\text{SiO}_4$ solution.....	15
2. Effluent profiles of pH and alkalinity from the slim tube injected with 0.087 N $\text{NaHCO}_3$ solution.....	16

## ILLUSTRATIONS (continued)

	<u>Page</u>
3. Effluent profiles for pH and alkalinity from the slim tube injected with 0.087 N Na <sub>2</sub> CO <sub>3</sub> solution.....	17
4. Decline of alkalinity in bottle test of reaction of Wilmington sand with 0.087 N alkali in synthetic Wilmington brine.....	18
5. Changes of pH in bottle test of reaction of Wilmington sand with 0.087 N alkali in synthetic Wilmington brine.....	19
6. Changes of pH in bottle test of reaction of Wilmington sand with 0.087 N alkali in synthetic Wilmington brine.....	20
7. Magnesium production in slim tube experiments.....	21
8. Calcium production in slim tube experiments.....	22
9. Sulfate production in slim tube experiments.....	23
10. Oil production in slim tube experiments.....	24
11. Brine permeability in slim tube experiments.....	25

## MINERAL-ALKALI REACTIONS UNDER DYNAMIC CONDITIONS

by Shawn D. Thornton and Philip B. Lorenz

---

### ABSTRACT

Three alkaline agents -- sodium orthosilicate, sodium carbonate, and sodium bicarbonate -- were injected into slim tubes packed with Wilmington (CA) sand containing synthetic Wilmington brine and Wilmington crude oil at waterflood residual saturation, and reservoir temperature, 52° C. The effluent solutions during 3 pore volumes of chemical injection and 1 pore volume of water drive were analyzed for calcium, magnesium, sulfate, total alkalinity, and pH. The transmission of all components was delayed, but to different degrees. Some of the results were interpreted in terms of solubilities of calcium and magnesium silicates and carbonates, and calcium sulfate. Known ionic equilibria were used to interpret the pH history for bicarbonate injection, and indicated a loss of carbon dioxide from the samples before analysis. The orthosilicate gave the best tertiary oil recovery, but bicarbonate was transmitted with much less loss, and showed promise of being a cost-effective agent when enhanced with dilute surfactant.

### INTRODUCTION

Alkaline flooding is probably the most difficult EOR process to model. There are at least three distinct mechanisms: IFT reduction, emulsification, and wettability alteration.<sup>1</sup> The mobilization process depends on pH, which is governed by an array of ionic equilibria, involving neutralization, precipitation, dissociation of weak polyprotic acids, dehydration, hydrolysis, polymerization (of silicates and phosphates), and complexation (sequestering). These equilibria are affected in turn by the solution-mineral interactions, which include adsorption,<sup>2</sup> ion exchange, dissolution, and precipitation. For minerals containing sulfur and iron, the mineral species can change with the oxidation-reduction conditions (Eh). One relatively neglected factor is that many reservoirs contain significant amounts of carbon dioxide partitioned between brine, oil, and any gas phase. This constitutes an acid capacity that must be neutralized by the injected alkali.

The problems are augmented by the wide variation of reaction rates. Ion exchange and neutralization are fast -- virtually instantaneous on a reservoir

time scale. Precipitation of divalent-ion carbonates and silicates is generally fast, although there is some evidence of an induction period<sup>3</sup> (delay in the onset of reaction) and metastable supersaturation.<sup>4</sup> The metamorphosis of aluminosilicates by solution-precipitation is not only slow but also appears to have a finite induction period.<sup>5</sup> The behavior of alkalis can be expected to be different under static and flowing conditions. For these reasons, the behavior of different alkaline agents is specific, not uniquely related to pH or alkaline capacity.

This report provides data on the individual differences between three alkalis in a particular oil/mineral system. Some of the differences have a ready explanation, and others suggest additional investigations that should be carried out to provide the basic understanding necessary for valid modeling.

Sodium orthosilicate was used by itself, but dilute surfactant was added to the weaker alkalis (sodium carbonate and sodium bicarbonate) to enhance oil mobilization. However, the primary emphasis of the work was on the reaction of the alkalis with brine and rock under flowing conditions.

#### ACKNOWLEDGMENTS

This research program was designed and performed by S. D. Thornton. The data analysis and writing are the work of P. B. Lorenz. Thanks are due to E. H. Mayer of THUMS Long Beach Co., who supplied the Wilmington sandstone and crude oil, and to Huang Ya-Duo of the Scientific Research Institute of Petroleum Exploration and Development, Beijing, China, who assisted in the experiments. The work was performed for the U. S. Department of Energy under cooperative agreement DE-FC22-83FE60149.

#### EXPERIMENTAL PROCEDURES

Three slim-tube experiments were conducted for measuring the displacement of ions through Wilmington reservoir sandstone. The compositions of the solutions used in this work are given in table 1. Three stainless steel slim tubes with an outer diameter of 0.25 in. (0.635 cm) and an inner diameter of 0.18 in. (0.457 cm) were assembled to a length of 60 ft (18.3 m). Each slim tube was packed with toluene-extracted Wilmington reservoir sand to a porosity

TABLE 1. - Compositions of solutions used in the slim-tube experiments

Solution	Component	Concentration, equiv kg <sup>-1</sup>
Simulated Wilmington brine	NaCl	0.404
	CaCl <sub>2</sub>	0.0300
	MgCl <sub>2</sub>	0.0248
NaHCO <sub>3</sub> solution	NaCl	0.318
	NaHCO <sub>3</sub>	0.0870
	NEODOL 25-3S <sup>1</sup>	0.024
Na <sub>2</sub> CO <sub>3</sub> solution	NaCl	0.316
	Na <sub>2</sub> CO <sub>3</sub>	0.0870
	NEODOL 25-3S <sup>1</sup>	0.023
Na <sub>4</sub> SiO <sub>4</sub> solution	NaCl	0.317
	Na <sub>4</sub> SiO <sub>4</sub>	0.0850

<sup>1</sup>NEODOL™ 25-3S is an anionic surfactant from Shell Development Co. with a formula weight of 437 g mol<sup>-1</sup>.

of 0.29 ± 0.01. The sand was obtained from well D492 at a depth of 4,665 ft. The sandpacks were saturated with simulated Wilmington brine (see table 1). Wilmington oil (viscosity, 60 cP at 52° C) was introduced into the slim tubes at a differential pressure of approximately 33 psi/ft (0.074 atm/cm), then the slim tubes were waterflooded at a rate of 0.2 to 0.3 PV/d (12 to 18 ft/d) with simulated Wilmington brine. After waterflooding, the solutions described in table 1 which contained NaHCO<sub>3</sub>, Na<sub>2</sub>CO<sub>3</sub>, and Na<sub>4</sub>SiO<sub>4</sub> were each injected into their respective slim tubes at a flowrate of 1.0 ± 0.2 pore volumes per month (2.0 ± 0.4 ft/d) and at differential pressures ranging from 1.0 psi/ft to 3.0 psi/ft (0.0022 to 0.0067 atm/cm). The effluent solutions were analyzed for elements by atomic absorption, for pH with a glass electrode, and for alkalinity by titration to pH 4 with 0.1 N HCl solution. Sulfate ion was measured indirectly by adding BaCl<sub>2</sub> to precipitate BaSO<sub>4</sub> under acidic conditions and measuring residual barium by atomic absorption. Temperature was maintained at the Wilmington reservoir temperature of 52° C for the oil saturation, waterflood, and alkali injection.

For comparison, bottle tests were conducted with the three alkalis (no surfactant) and Wilmington sand. In each test, the sand was mixed with 0.087 N alkaline solution at a solid-liquid ratio of 1.1:1 (wt/wt). The bottles were placed in an unstirred water bath at 52° C and were shaken by hand at least once daily. Aliquots of the supernatant were removed periodically and analyzed for alkalinity, pH, and sulfate.

## RESULTS

### Alkalinity and pH

The data of Somerton and Radke<sup>6</sup> indicate that the ion exchange for Wilmington sand is about 10 meq/kg for acid sites and 5 meq/kg for divalent sites. In the present experiments, one pore volume (0.15 dm<sup>3</sup>/kg) of the injected solutions contained 49 meq of alkalinity per kg of sand. Ion exchange should therefore consume 0.3 PV.

The effluent profiles in figures 1 through 3 show the individuality of responses to the different alkaline agents.

### Orthosilicate

The alkalinity and pH curves are both delayed by about 1.3 PV. This indicates a "fast reaction," but in excess of what could reasonably be ascribed to ion exchange. Possibly a rapid solution-precipitation reaction involving magnesium silicate contributed to the lag. The increase in alkalinity was more gradual than the increase in pH, but the decline was faster. Analysis for silicon in this experiment revealed that the injected silicate appeared in the effluent only after 2.5 PV, indicating that some other alkaline species was generated by interaction of the orthosilicate with the sand.

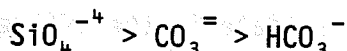
### Bicarbonate

There is about a 0.2 PV lag in both alkalinity and pH curves, which is a plausible chromatographic delay for ion exchange. The effluent leveled off at the injected value for both quantities; however, the alkalinity curve indicates some consumption that is slow but finite.

## Carbonate

The irregular curves suggest a delay of about 0.5 PV (presumably due to ion exchange plus some fast dissolution-precipitation), and then a slower consumption reaction that has an induction period. The effluent alkalinity reached its injected value, but the pH leveled off at 1.2 units below the injected value. With all three alkalis, the effluent pH showed an initial decrease followed by an abrupt increase at the end of the fast (ion exchange) reaction.

The behavior of the three agents in bottle tests is shown in figures 4 through 6. There was an immediate drop in alkalinity on contact of the solution with mineral, and a continuing slow decline. The extent of the decrease was in the order



as observed in the flow experiments. The pH behavior displayed some qualitative differences. The carbonate solution showed a large initial drop, and the bicarbonate pH showed an increase. For a simple neutralization of alkali, the pH should follow the same course as that in a titration curve. The silicate was indeed near one of its buffer points (pH 11.7), and its slow pH change is expected. The carbonate ion traversed its buffer point (pH 9.5) before slowing down, and bicarbonate was between buffer points (pH 9.5 and 6.0), where pH should be most sensitive to neutralization. A possible cause of these anomalies in the presence of sand is the formation of complexes<sup>7</sup> such as  $\text{MgHCO}_3^+$  that alter pH without affecting alkalinity. This is related to the discrepancy between silicate concentration and alkalinity in figure 1, and is a subject that merits further investigation.

Figure 6 shows that the decline of pH for silicate and carbonate was reduced in the presence of oil.

## Magnesium and Calcium

Magnesium in the effluent (fig. 7) started out at its concentration in the waterflood brine. Calcium (fig. 8) was almost three times the original concentration. The most obvious explanation for the surplus is the presence of gypsum. The production of sulfate shown in figure 9 makes this more plausible. For the first pore volume of effluent

$$[\text{Ca}^{++}] = 4.1 \times 10^{-2} \text{ mol/kg}$$

$$[\text{SO}_4^{=}] = 2.8 \times 10^{-2} \text{ mol/kg}$$

The mean activity coefficient  $\gamma_{\pm}$  of  $\text{CaSO}_4$  is 0.150,<sup>7</sup> and the product

$$\gamma_{\pm}^2 [\text{Ca}^{++}][\text{SO}_4^{=}] = 2.6 \times 10^{-5}$$

which is equal to the literature value.<sup>8</sup> However, some other data do not fit the assumption that gypsum is responsible. In the bottle tests, as shown in table 2, the sulfate concentration in the presence of strong alkalis was about the same as that in the slim-tube effluent before the alkali reached the outflow end, although solubility product considerations would predict a much higher value. The decline of sulfate in the effluent on the appearance of the alkali contradicts both our expectations and the bottle test results. A possible hypothesis is that alkali deposits an insoluble precipitate that prevents further dissolution of gypsum. This would also explain the slow buildup of sulfate (table 2) in the presence of silicate, which gives a more flocculent precipitate. However, it should be mentioned that gypsum has not been detected in Wilmington sand, and sulfate is not present in Wilmington brine. This aspect of the present results needs further investigation.

It is also difficult to explain why the magnesium concentration in the slim-tube effluent began to decline immediately when alkali was injected.

Other features of the results in figures 7 and 8 are more amenable to explanation:

1. The displacement of the calcium production curves with carbonate and silicate is due to the delay in the first arrival of the alkali (figures 1 and 3). Bicarbonate was delayed very little, and so reduces calcium concentration at an earlier stage.

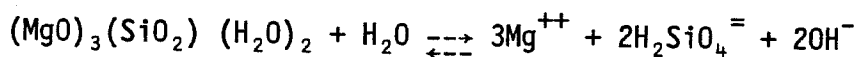
TABLE 2. - Sulfate concentrations in bottle-test supernatants. The solid-liquid ratio is 1.1 kg sandstone/kg solution, and the temperature is 52° C.

Solution	[SO <sub>4</sub> <sup>2-</sup> ] after 28 hr, mol kg <sup>-1</sup>	[SO <sub>4</sub> <sup>2-</sup> ] after 1610 hr, mol kg <sup>-1</sup>
0.084 N NaOH	0.0238	0.0286
0.085 N Na <sub>4</sub> SiO <sub>4</sub>	0.0167	0.0261
0.087 N Na <sub>2</sub> CO <sub>3</sub>	0.0230	0.0271
0.087 N NaHCO <sub>3</sub>	0.0202	0.0241

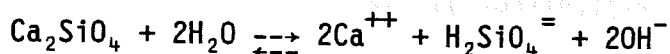
2. The magnesium concentration declined earliest on injection of silicate, probably because magnesium silicate is highly insoluble.

Solubility products at 25°:

Chrysotile,<sup>9</sup> 10<sup>-39</sup>



Calcium silicate,<sup>10</sup> >10<sup>-8</sup>



3. The shoulder on the carbonate and bicarbonate curves in figure 7 may be due to the solubility of MgCO<sub>3</sub>. At this point we find [Mg<sup>++</sup>] = 4.4 X 10<sup>-3</sup>. For carbonate injection, with measured pH 8.0 (fig. 2), the system should be 96% HCO<sub>3</sub><sup>-</sup>, so [CO<sub>3</sub><sup>=</sup>] = 0.04 (0.087/2) = 1.7 x 10<sup>-3</sup>, and [Mg<sup>++</sup>][CO<sub>3</sub><sup>=</sup>] = 0.7 X 10<sup>-5</sup>. For bicarbonate injection with measured pH 8.2 (fig. 3), the system should be 6% CO<sub>3</sub><sup>=</sup>, so [Mg<sup>++</sup>][CO<sub>3</sub><sup>=</sup>] = (0.0044)(0.06)(0.087) = 2.3 X 10<sup>-5</sup>. Comparing with the solubility product 2.6 X 10<sup>-5</sup> (not corrected for activity),<sup>10</sup> this explanation is possible but not compelling. These order-of-magnitude calculations gloss over the substantial covalent ion pairing between magnesium and carbonate and the fact that the solid is probably a mixed, dolomitic crystal rather than simple magnesite.

## The Role of Carbon Dioxide

For a bicarbonate-carbonic acid system at pH below about 8, the equilibrium partial pressure of  $\text{CO}_2$  exceeds the partial pressure in the atmosphere. If effluent samples are not confined, the escape of  $\text{CO}_2$  can lead to spurious analytical results. For a closed system, pH can be calculated from the measured quantities: alkalinity and calcium concentration (assuming that calcium is solely responsible for precipitation). This calculation was carried out for the slim tube experiment in which  $\text{HCO}_3^-$  was injected. The parameters employed are listed in table 3. Measured calcium is

$$[\text{Ca}] = [\text{Ca}^{++}] + [\text{CaHCO}^+]$$

Measured alkalinity is

$$A = 2[\text{CO}_3^{=}] + [\text{HCO}_3^-]$$

Stoichiometry and solution equilibria give

$$[\text{Ca}^{++}] = \gamma_3[\text{Ca}] / (K_3\gamma_{\text{Ca}}\gamma_2[\text{HCO}_3^-] + \gamma_3)$$

$$[\text{CO}_3^{=}] = \gamma_2 K_1 A / (\gamma_1 \gamma_{\text{H}}[\text{H}] + 2\gamma_2 K_1)$$

Rearranging,

$$\text{pH} = -\log(\gamma_{\text{H}}[\text{H}^+]) = (\gamma_2 K_1 / \gamma_1) ((A / [\text{CO}_3^{=}]) - 2)$$

Taking account of mineral-solution equilibrium,

$$[\text{CO}_3^{=}] = \frac{K_4(\gamma_2 K_3 A [\text{Ca}] + \gamma_3)}{\gamma_{\text{Ca}}(\gamma_1 \gamma_3 [\text{Ca}] + 2\gamma_2 K_3 K_4)}$$

TABLE 3. - Parameters used in calculations of pH

Equilibrium constants at 24°		Reference
$\text{HCO}_3^- \rightleftharpoons \text{H}^+ + \text{CO}_3^{=}$	$K_1 = 4.47 \times 10^{-11}$	15
$\text{CO}_2 + \text{H}_2\text{O} \rightleftharpoons \text{H}^+ + \text{HCO}_3^-$	$K_2 = 4.37 \times 10^{-7}$	16
$\text{Ca}^{++} + \text{HCO}_3^- \rightleftharpoons \text{CaHCO}_3^+$	$K_3 = 1.17 \times 10^1$	8
$\text{CaCO}_3 \rightleftharpoons \text{Ca}^{++} + \text{CO}_3^{=}$	$K_4 = 3.39 \times 10^{-9}$	8
$\text{CO}_2 (\text{aq}) \rightleftharpoons \text{CO}_2 (\text{gas})$	$h = 3.1 \times 10^{-2} \text{ mol/kg}^{-1}/\text{atm}^{-1}$	17

Activity coefficients at 52°		
$\text{CO}_3^{=}$	$\gamma_1 = 0.230$	8
$\text{HCO}_3^{=}$	$\gamma_2 = 0.693$	8
$\text{CaHCO}_3^+$	$\gamma_3 = 0.693$	8
$\text{H}^+$	$\gamma_4 = 0.765$	8
$\text{Ca}^{++}$	$\gamma_{\text{Ca}} = 0.261$	8

The results in table 4 show that pH so calculated is much lower than the measured value. The  $\text{CO}_2$  content is calculated from

$$[\text{CO}_2] = (\gamma_2 A / K_2) 10^{-\text{pH}}$$

assuming that  $\gamma_{\text{CO}_2} \approx 1$ . Since many of the partial pressures in table 3 are higher than the atmospheric value of  $3 \times 10^{-4}$ , it is quite plausible that the pH deviation is a result of evaporation. After the first pore volume injected, there is a linear relation between calculated  $P_{\text{CO}_2}$  and the discrepancy between calculated and measured pH, with a correlation coefficient of 0.99.

TABLE 4. - Calculated vs. measured pH of effluent from slim tube with injection of  $\text{NaHCO}_3$

Pore Vol, injected <sup>1</sup>	Alkalinity, meq/kg	[Ca], m-mol/kg	pH meas.	pH calc.	[CO <sub>2</sub> ], m-mol/kg	P <sub>CO<sub>2</sub></sub> , atm	ΔpH
0.27	4.4	41.7	7.87	6.36	3.0	.10	1.51
0.71	4.1	41.3	7.63	6.39	2.6	.08	1.24
0.88	4.3	39.2	7.65	6.40	2.7	.09	1.25
1.08	15.2	8.29	7.58	6.52	7.3	0.24	1.06
1.23	52.6	0.177	8.23	7.66	1.8	0.06	0.57
1.40	71.4	0.261	8.18	7.35	5.1	0.16	0.83
1.60	73.5	0.262	8.26	7.36	5.3	0.17	0.92
1.78	76.6	0.425	8.26	7.11	9.4	0.30	1.15
1.98	77.6	0.576	8.32	6.97	13.2	0.43	1.35
2.17	79.4	0.614	8.38	6.93	14.8	0.48	1.45
2.36	80.5	0.451	8.38	7.06	11.1	0.36	1.32
2.57	81.8	0.554	8.40	6.97	13.9	0.45	1.43

<sup>1</sup>These values are the fraction of the brine pore volume, calculated at each point in the flow from oil saturation derived from figure 10.

The neglect of the effect of magnesium complexation<sup>11-12</sup> of  $\text{CO}_3^{2-}$  on the effective alkalinity or any tendency toward metastable supersaturation of  $\text{CaCO}_3$ <sup>4</sup> would also cause deviations in the same direction. It is evident that for legitimate modeling of an alkali process with carbonate and bicarbonate, data on pH and alkalinity should be obtained on protected samples, preferably at reservoir temperature and pressure.

### Oil Production and Permeability

Tertiary oil production curves are presented in figure 10. Table 5 gives the results in terms of recovery efficiency. The surfactant-sodium carbonate combination was less effective than the orthosilicate. In view of results published elsewhere,<sup>13,14</sup> this indicates that the surfactant-alkali slug was not well optimized. The sodium bicarbonate-surfactant ultimately released as much oil as sodium carbonate-surfactant, but recovery was slower. As shown in

TABLE 5. - Oil production in slim-tube experiments

Injected alkali	Porosity	$S_{oi}$	$S_{ow}^1$	$S_{oc}^2$	Tertiary recovery, %
Sodium orthosilicate	0.26	0.78	0.18	0.08	54
Sodium carbonate	0.27	0.75	0.18	0.115	36
Sodium bicarbonate	0.28	N.D.	0.18	0.12	34

<sup>1</sup>Determined collectively for all three tubes.

<sup>2</sup>Oil saturation after 3 PV chemical slug and 1 PV water drive.

figures 2 and 3, the difference in rates developed at a time when the effluent pH values were very similar. It is possible that the bicarbonate recovery was hampered by the permeability effects shown in figure 11. Brine permeability shows a distinct decrease with bicarbonate. The effective permeability with carbonate was erratic, but exhibited no trend. The effective permeability with silicate shows a possible increase. The permeability trends are in the same order as the oil recovery. It is quite implausible to attribute permeability changes to mineral precipitation. Wettability changes could be responsible for the permeability behavior, with bicarbonate making the system more water wet. The behavior with silicate could be caused by increased oil wettability or mineral dissolution; however, it is noteworthy that some emulsion was observed in the effluent at the time of the large increase in effective permeability near 2 pore volumes injected. One would expect elimination of an emulsion to cause an increase in effective permeability.

### CONCLUSIONS

1. Sodium bicarbonate undergoes little reaction with the Wilmington sand. The results show a slow consumption reaction, but it was very limited in scope.
2. Sodium bicarbonate ultimately displaces as much oil as sodium carbonate (both enhanced with surfactant but not optimized).

3. All alkalis reduce divalent ion content of brine, which will suppress degradation of co-injected surfactant. Silicate was most effective for magnesium, and bicarbonate was most effective for calcium, under the conditions of these experiments.
4. Bicarbonate reaches its full alkalinity after considerably fewer pore volumes than carbonate, which requires fewer pore volumes than orthosilicate.
5. Effluent samples should be confined to prevent loss of  $\text{CO}_2$ , to prevent misleading results in carbonate/bicarbonate floods.

#### RECOMMENDATIONS FOR FUTURE RESEARCH

Several unanswered questions suggest further work that would improve our understanding of alkaline flooding.

1. What fast reactions occur in addition to ion exchange?
2. What is the reason for the nonequivalence of pH and alkalinity changes?
3. Why did the effluent from the sodium carbonate injection fail to attain the pH of the injected slug (and why did the pH drop so markedly in the bottle test?)
4. What caused the anomalies in the data that were attributed to gypsum dissolution?
5. What caused the early decline of magnesium in the effluent? (There was a similar anomaly with surfactant production, not presented.)
6. What is the relative importance of the loss of  $\text{CO}_2$  before analysis and supersaturation of calcite and/or dolomite?
7. What caused the shoulder of the magnesium production curves?

8. What was the relative influence or wettability, emulsification, and mineral dissolution of the permeability changes?

#### REFERENCES

1. Mayer, E. H., R. L. Berg, J. D. Carmichael, and R. M. Weinbrandt. Alkaline Injection for Enhanced Oil Recovery -- A Status Report. *J. Pet. Tech.*, v. 35, No. 1, January 1983, p. 209.
2. Thornton, S. D. and C. J. Radke. Dissolution and Condensation Kinetics of Silica in Alkaline Solution. Pres. at the SPE 1985 California Regional Meeting, Bakersfield, Mar. 27-29. SPE paper 13601.
3. Stamper, R. Physicochemical Investigations of the Precipitation of Calcium Carbonate from Water. *Angew. Chem.*, v. 48, No. 7, 1935, pp. 117-124.
4. Patton, J. T. CO<sub>2</sub> Formation Damage Study, Final Report. U.S. Department of Energy Report No. DOE/MC/10865-13, July 1983.
5. Thornton, S. D. and P. B. Lorenz. Role of Silicate and Aluminate Ions in the Reaction of Sodium Hydroxide with Reservoir Minerals. Pres. at the SPE Int. Symp. on Oilfield Chemistry, San Antonio, TX, Feb. 4-6, 1987. SPE paper 16277.
6. Somerton, W. H., and C. J. Radke. Role of Clays in the Enhanced Recovery of Petroleum. Pres. at the First Joint SPE/DOE Symposium on Enhanced Oil Recovery, Tulsa, OK, Apr. 20-23, 1980. SPE/DOE paper no. 8845.
7. Culberson, C. H., G. Latham, and R. G. Bates. Solubilities and Activity Coefficients of Calcium and Strontium Sulfates in Synthetic Seawater at 0.5 and 25° C. *J. Phys. Chem.*, v. 82, No. 25, 1978, p. 2693.
8. Plummer, L. N. and E. Busenberg. The Solubilities of Calcite, Aragonite and Vaterite in CO<sub>2</sub>-H<sub>2</sub>O Solutions Between 0 and 90° C, and an Evaluation of the Aqueous Model for the System CaCO<sub>3</sub>-CO<sub>2</sub>-H<sub>2</sub>O. *Geochim. et Cosmochim. Acta*, v. 46, 1982, p. 1011.
9. Hostetler, P. B. and C. L. Christ. Studies in the System MgO-SiO<sub>2</sub>-CO<sub>2</sub>-H<sub>2</sub>O(I): The Activity-Product Constant of Chrysotile. *Geochim. et Cosmochim. Acta*, v. 32, 1968, p. 485.
10. Handbook of Chemistry and Physics, 20th (1935) and 47th (1967) Editions. Chemical Rubber Publishing Co., Cleveland, OH.
11. Garrels, R. M., M. E. Thompson, and R. Siever. Control of Carbonate Solubility by Carbonate Complexes. *Am. J. of Science*, v. 259, 1961, pp. 24-25.

12. Garrels, R. M. and M. E. Thompson. A Chemical Model for Sea Water at 25° C and One Atmosphere Total Pressure. Am. J. Sci., v. 260, 1962, pp. 57-66.

13. Shuler, P. J., R. M. Lerner and D. L. Kuehne. Improving Chemical Flooding Efficiency with Micellar/Alkaline/Polymer Processes. Pres. at the SPE/DOE Fifth Symp. on Enhanced Oil Recovery, Tulsa, OK, Apr. 20-23, 1986, SPE/DOE Paper No. 14934.

14. Lin, F. F. J., G. J. Besserer, and M. J. Pitts. Laboratory Evaluation of Crosslinked Polymer and Alkaline-Polymer-Surfactant Flood. J. Canadian Pet. Tech., November-December 1987, pp. 54-65.

15. Patterson, C. S., R. H. Busey, and R. E. Mesmer. Second Ionization of Carbonic Acid in NaCl Media to 250° C. J. Solution Chem., v. 13, No. 9, 1984, p. 647.

16. Patterson, C. S., G. H. Slocum, R. H. Busey, and R. E. Mesmer. Carbonate Equilibria in Hydrothermal Systems: First Ionization of Carbonic Acid in NaCl Media to 300° C. Geochim. et Cosmochim. Acta, v. 46, 1982, p. 1653.

17. Harned, H. S. and R. Davis, Jr. The Ionization Constant of Carbonic Acid in Water and the Solubility of Carbon Dioxide in Water and Aqueous Salt Solutions from 0 to 50° C. J. Am. Chem. Soc., v. 65, October 1943, p. 2030.

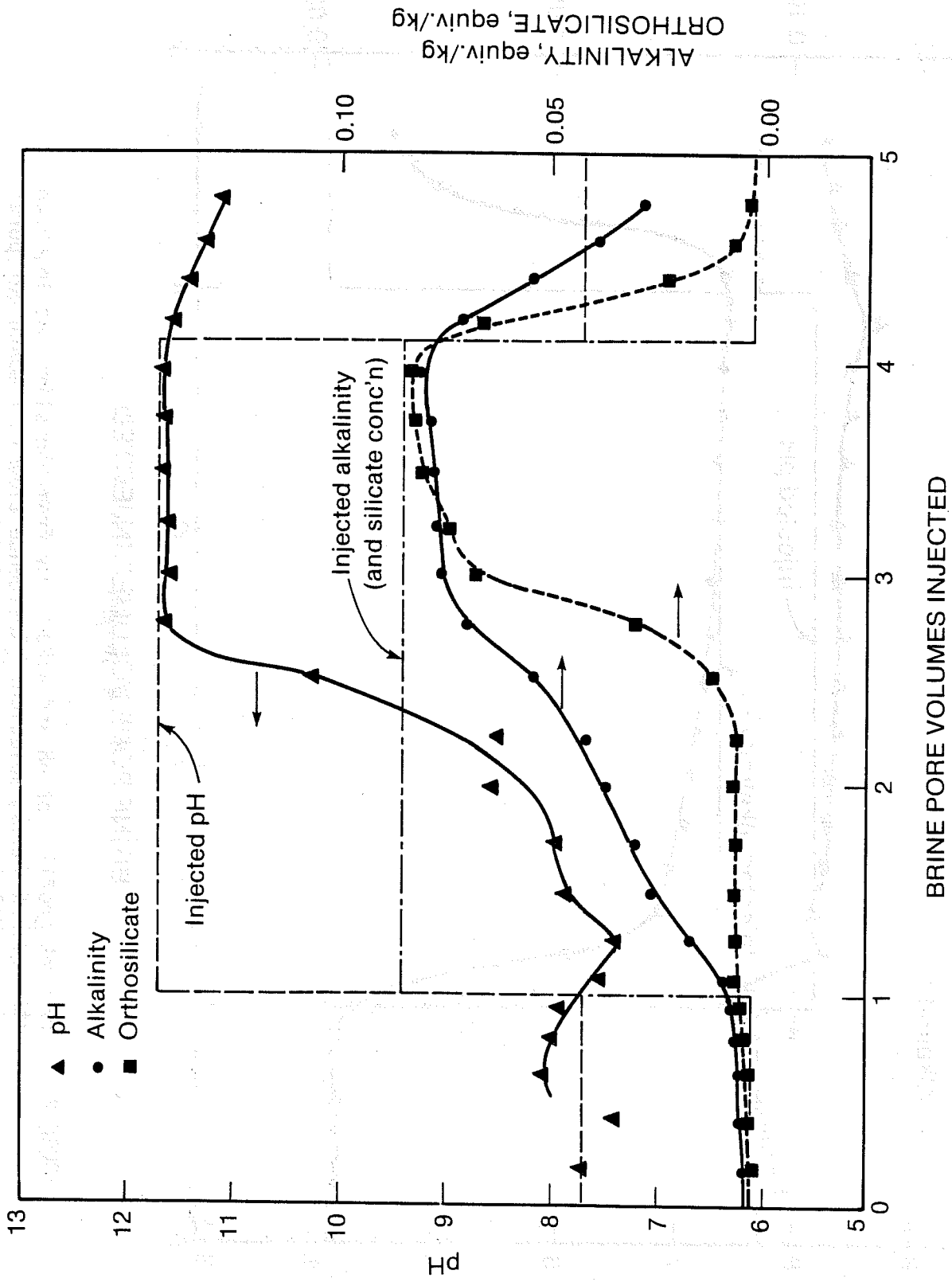


FIGURE 1. - Effluent profiles of pH and alkalinity from the slim tube injected with 0.085 N  $\text{Na}_4\text{SiO}_4$  solution. Residence time is 1 month per pore volume. Wilmington oil and sand at 52° C.

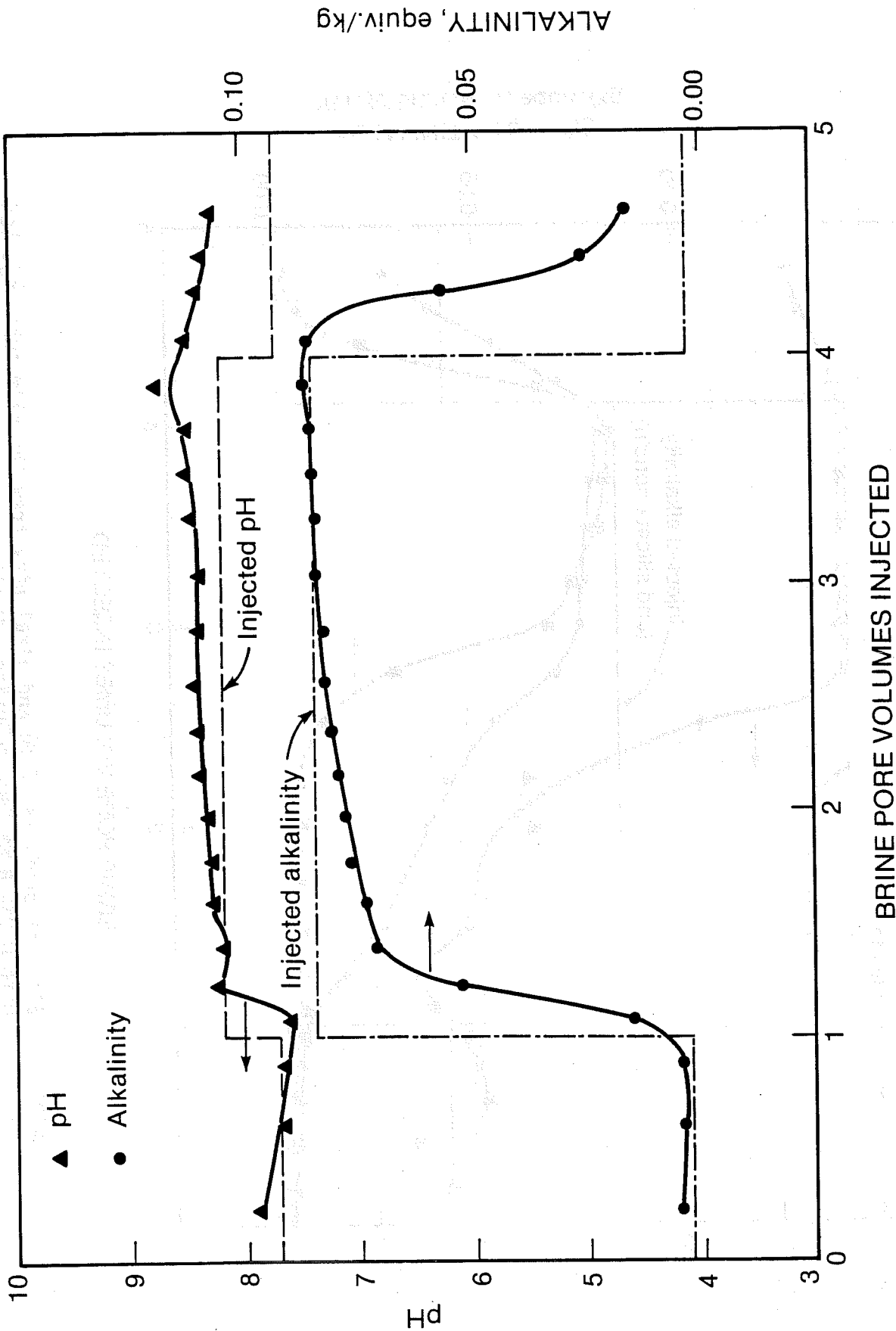


FIGURE 2. - Effluent profiles of pH and alkalinity from the slim tube injected with 0.087 N NaHCO<sub>3</sub> solution. Residence time is 1 month per pore volume. Wilmington oil and sand at 52° C.

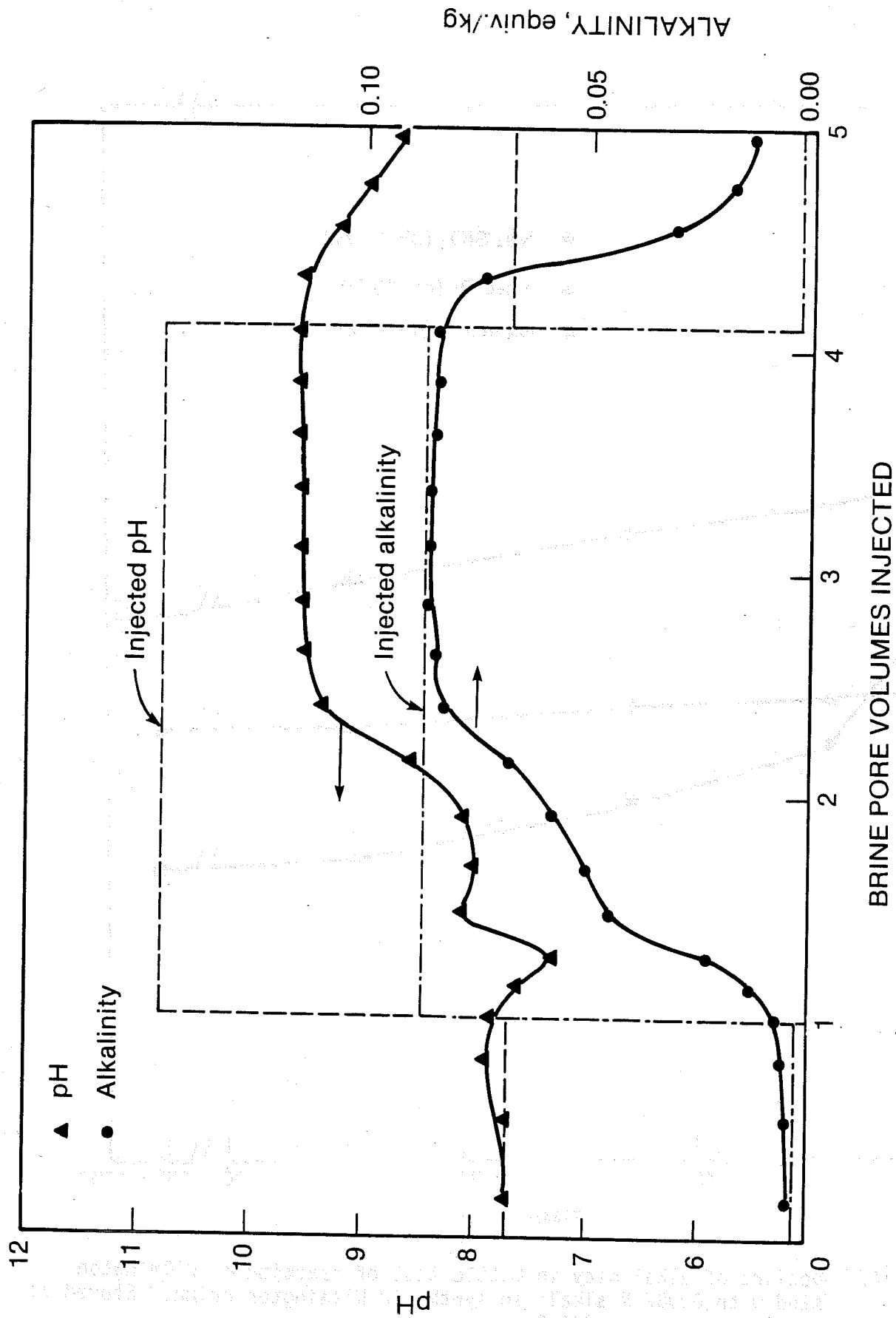


FIGURE 3. - Effluent profiles for pH and alkalinity from the slim tube injected with 0.087 N Na<sub>2</sub>CO<sub>3</sub> solution. Residence time is 1 month per pore volume. Wilmington oil and sand at 52° C.

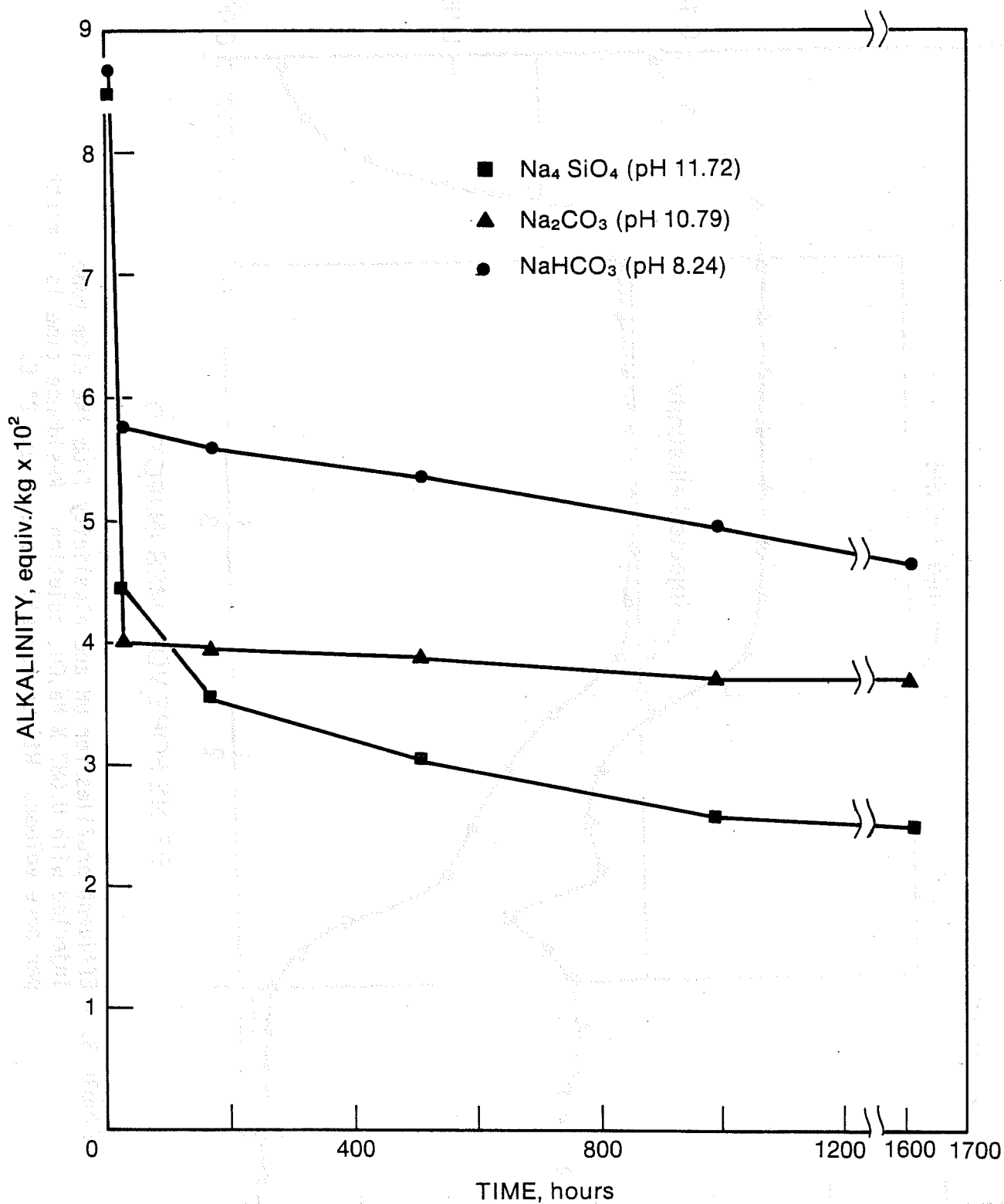


FIGURE 4. - Decline of alkalinity in bottle test of reaction of Wilmington sand with 0.087 N alkali in synthetic Wilmington brine. Stored at 52° C, measured at 24° C.

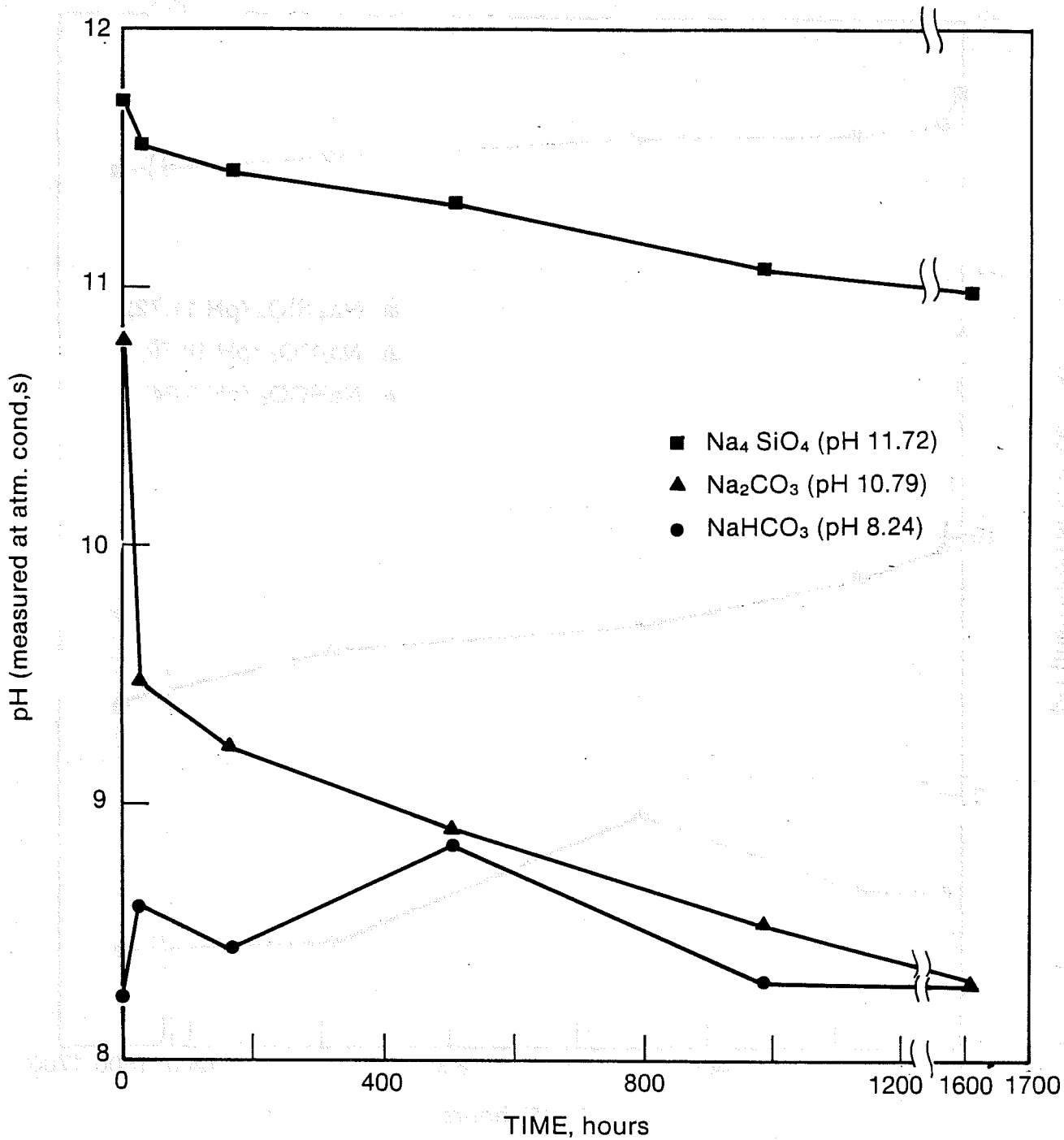


FIGURE 5. - Changes of pH in bottle test of reaction of Wilmington sand with 0.087 N alkali in synthetic Wilmington brine at 52° C.

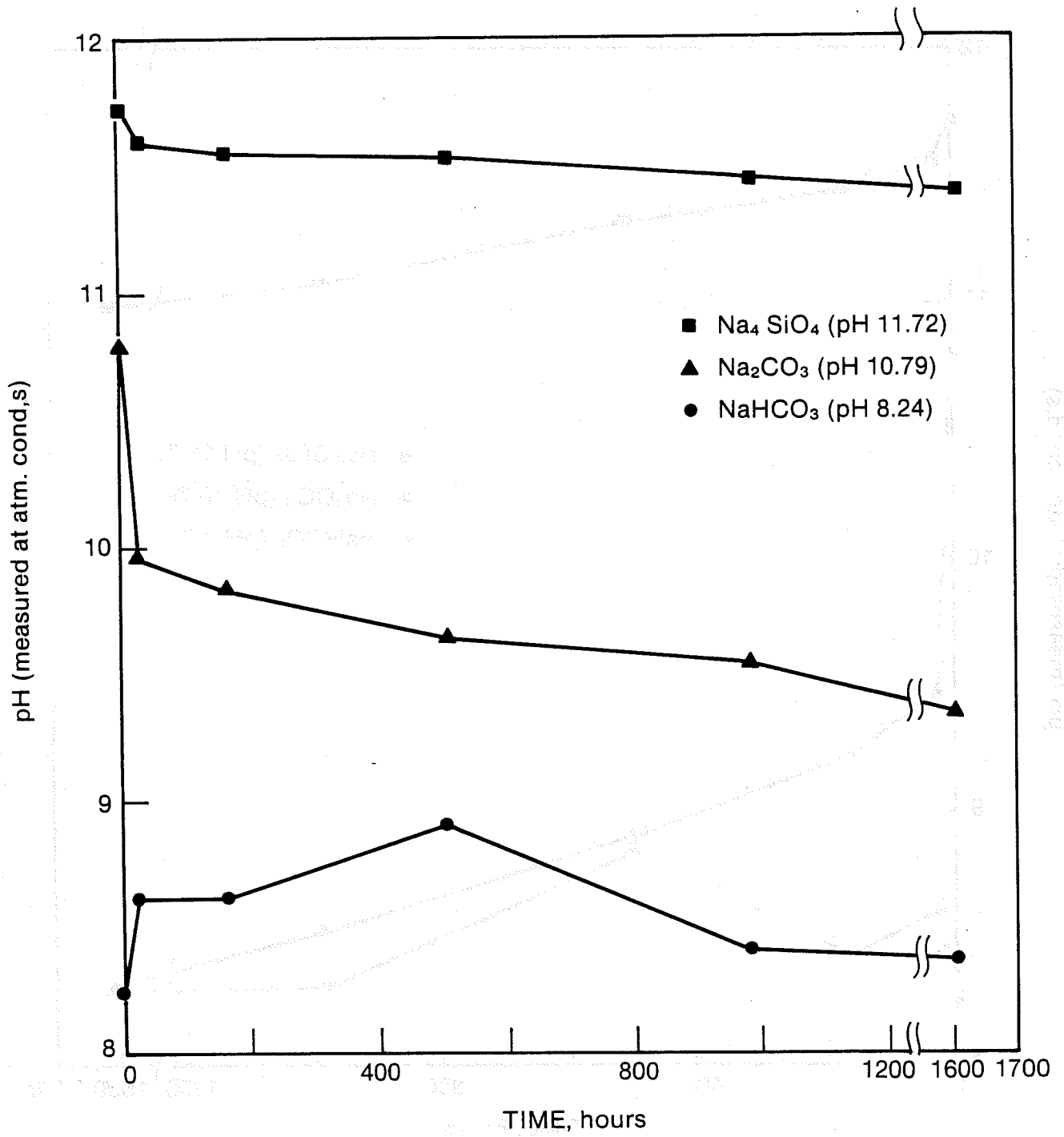


FIGURE 6. - Changes of pH in bottle test of reaction of Wilmington sand with 0.087 N alkali in synthetic Wilmington brine at 52° C.

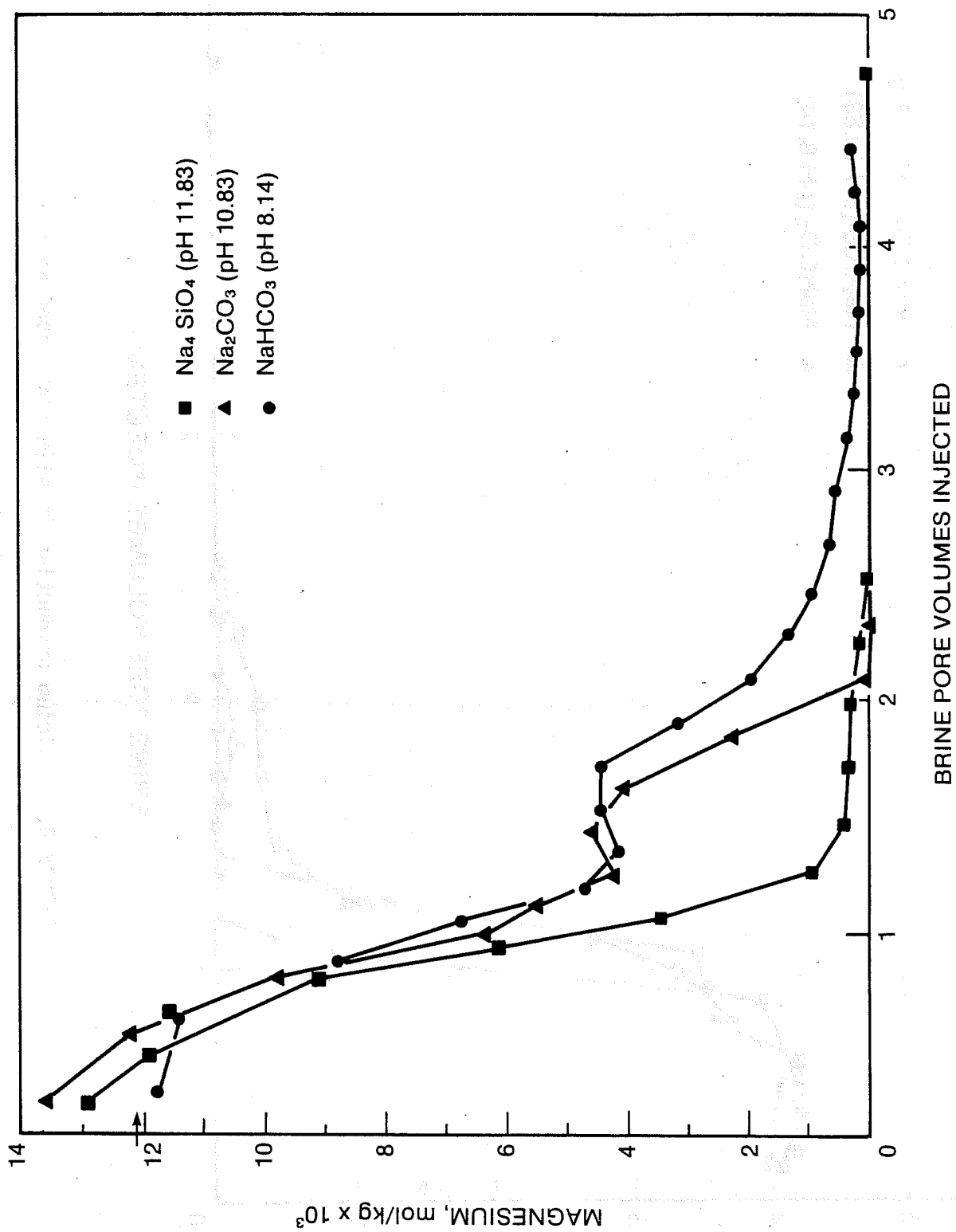


FIGURE 7. - Magnesium production in slim tube experiments.

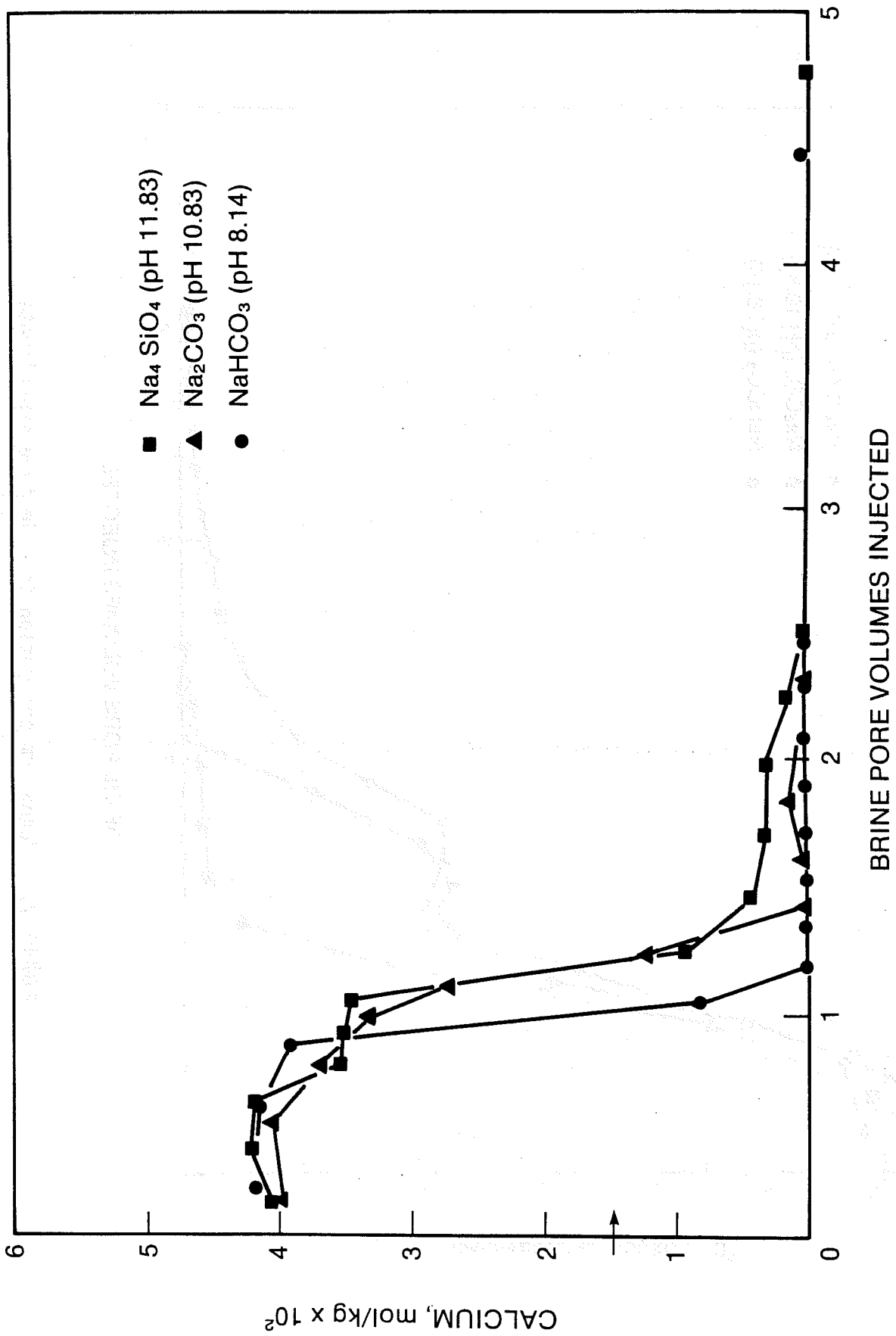


FIGURE 8. - Calcium production in slim tube experiments.

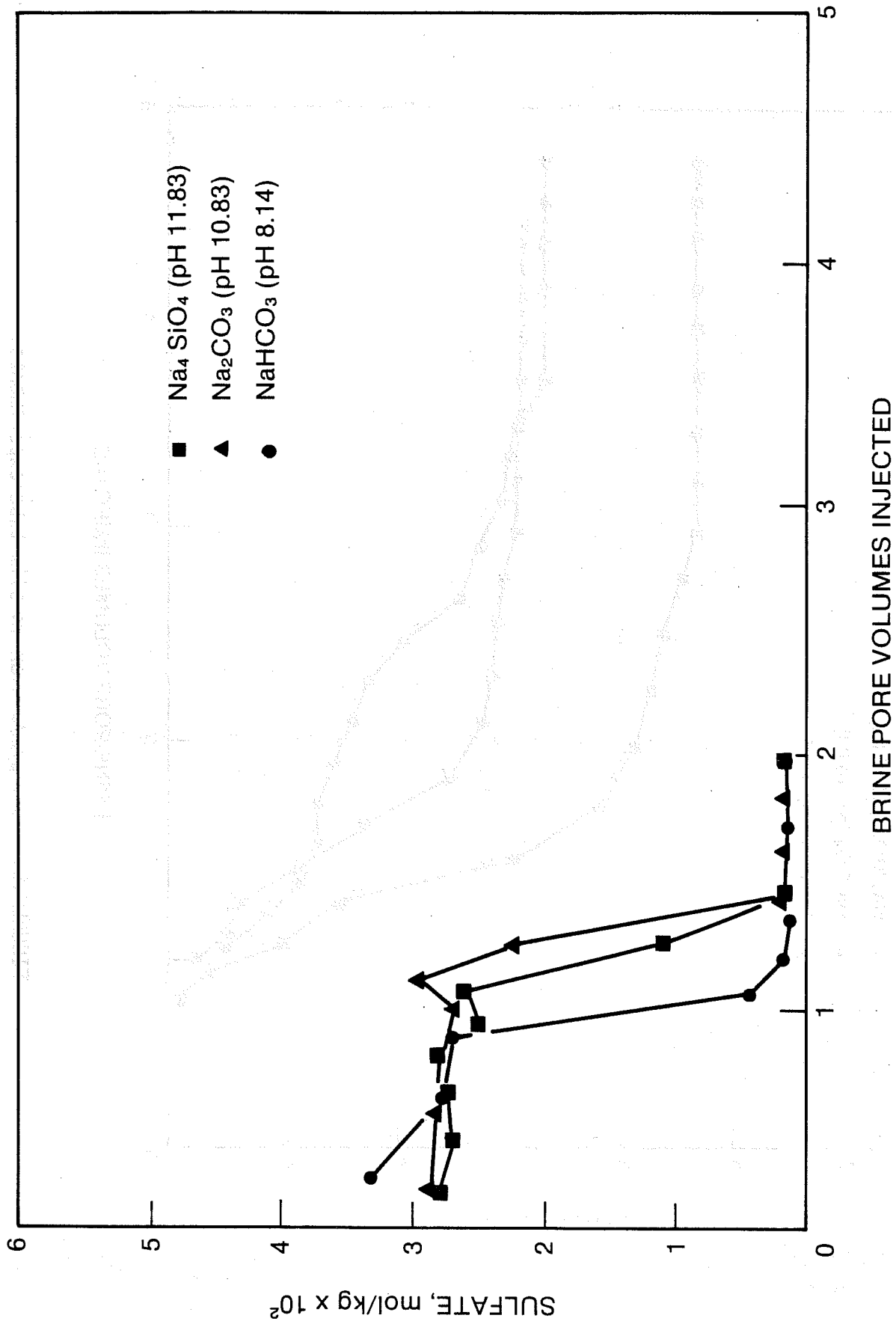


FIGURE 9. - Sulfate production in slim tube experiments.

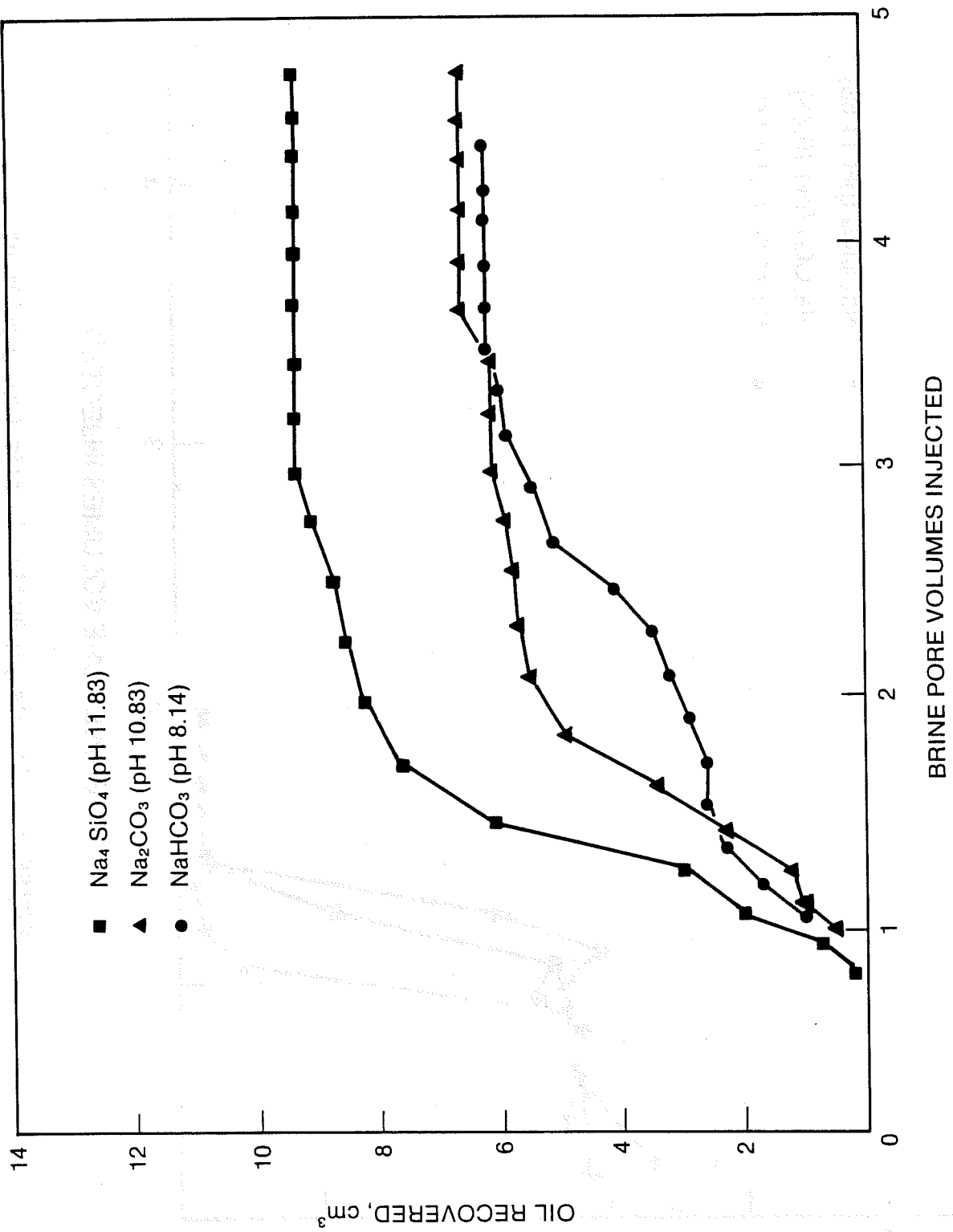


FIGURE 10. - Oil production in slim tube experiments.

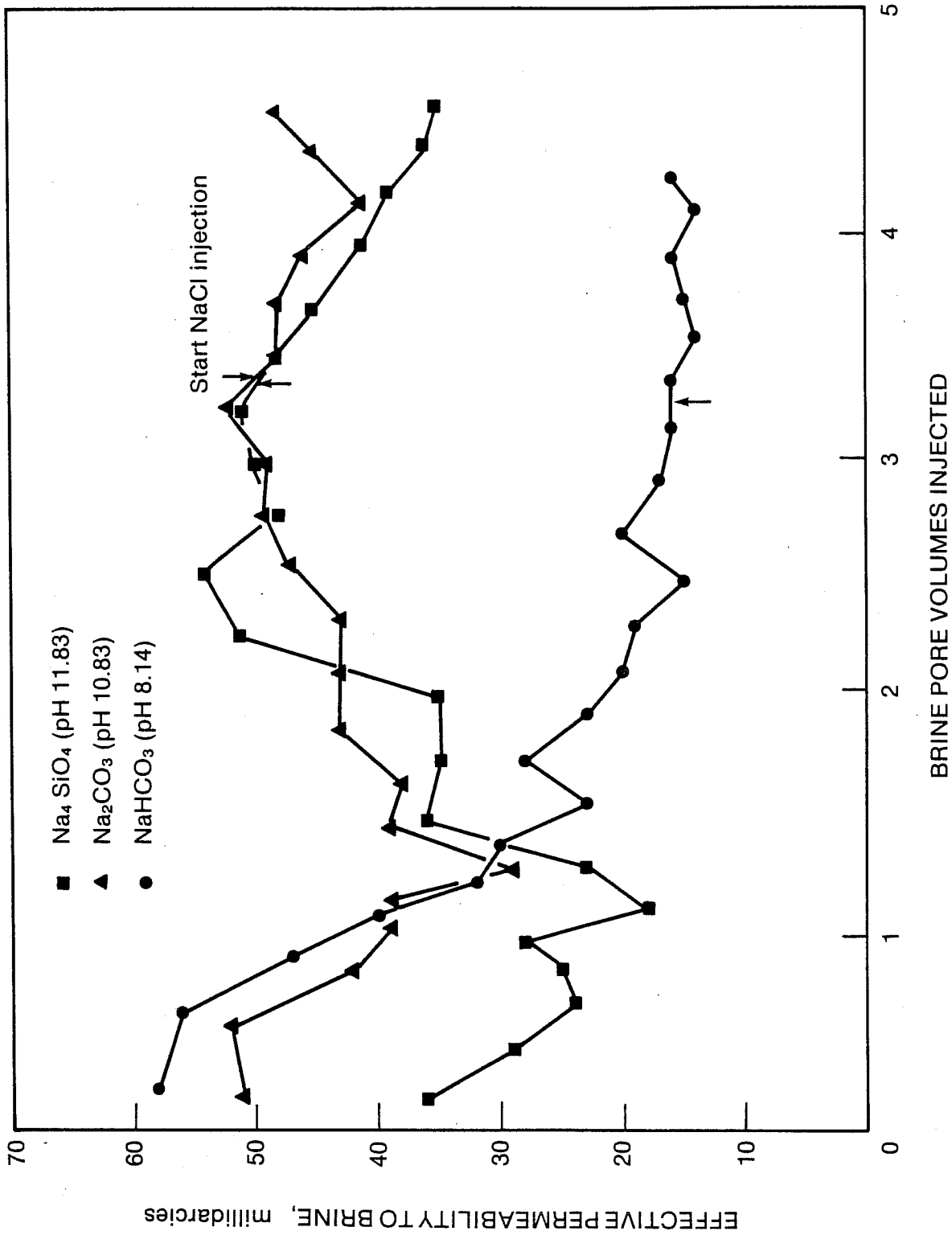


FIGURE 11. - Brine permeability in slim tube experiments.

